Investigation on the Mechanism of the Synthesis of Gold (I) Thiolate Complexes by NMR

ARTICLE *in* THE JOURNAL OF PHYSICAL CHEMISTRY C · APRIL 2014

Impact Factor: 4.77 · DOI: 10.1021/jp501020k

THE JOURNAL OF PHYSICAL CHEMISTRY C

Article

pubs.acs.org/JPCC

Investigation on the Mechanism of the Synthesis of Gold(I) Thiolate Complexes by NMR

Chunhong Yu,[†] Lili Zhu,[†] Rongchun Zhang,[‡] Xiaoliang Wang,*[,†] Chengchen Guo,[†] Pingchuan Sun,[‡] and Gi Xue*[,†]

[†]Department of Polymer Science and Engineering, Key Laboratory of High Performance Polymer Materials and Technology, Ministry of Education, School of Chemistry and Chemical Engineering, Nanjing University, Nanjing 210093, People's Republic of China

[‡]Key Laboratory of Functional Polymer Materials, Ministry of Education, College of Chemistry and School of Physics, Nankai University, Tianjin 300071, People's Republic of China

Supporting Information

ABSTRACT: In this article, we characterized the polymeric gold(I) thiolates that precipitated from the intermediate solutions during the synthesis process of gold nanoparticles (GNPs) by the Brust−Schiffrin two-phase method and investigated the formation mechanism of the polymeric gold(I) thiolates. The solution ^{1}H NMR confirmed the complete reduction from Au(III) to Au(I) with the addition of the first two equivalents of thiols, while only the third and fourth equivalents of thiols were found to participate in forming gold(I) thiolates. Gold(I) thiolates, $[Au(I)SR]_n$, precipitated from these solutions were further characterized by ^{1}H solid-state NMR spectroscopy under fast magic angle spinning (MAS), Raman spectroscopy, and thermogravimetric analysis. Further quantitative studies revealed that the composition of $[Au(I)SR]_n$ could be controlled by changing the order of addition of the third and fourth equivalents of thiols. This work has great significance to better understand the mechanism of gold nanoparticle formation and thus to tailor the properties of the final products.

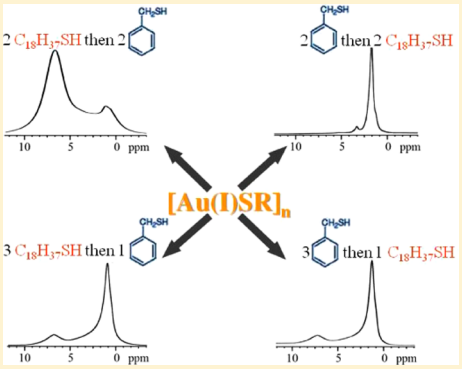

INTRODUCTION

Since the synthesis of monodispersed gold nanoparticles (GNPs) by the Brust−Schiffrin method (BSM),[1] much attention has been focused on the GNPs for their optical, electronic, catalytic, and biomedical properties and small size effect.[2−7] The preparation of GNPs plays a very important role in controlling the properties of resulting GNPs. In the process of studying the mechanism of GNP formation by the BSM, the polymeric gold(I)−alkanethiolates $[Au(I)SR]_n$ have attracted much interest for their special properties.[8−10] It is known that the unique characteristics of $[Au(I)SR]_n$, such as luminescent and catalytic properties, are essentially dependent upon their special compositions and structures. Great effort has been devoted to achieve detailed descriptions of such metal complexes.[10−15] Schaaff et al. have proved that large quantities of water and polar solvents (methanol, ethanol, THF) could promote the formation of $[Au(I)SR]_n$.[12] Recently, Tong et al. have clarified that, only when the aqueous layer was removed before adding the thiol, $[Au(I)SR]_n$ formed as the intermediate Au(I) precursor in the BSM.[15−18] Cha et al. investigated the temperature-dependent thermal/structural behavior of photoluminescent $[Au(I)SR]_n$ and demonstrated the relation between their thermal transition temperatures (the melting and decomposition temperatures) and the length of alkyl groups.[14] In addition, $[Au(I)SR]_n$ can also serve as gold precursors to get novel GNPs.[19−25] Negishi et al. reported the synthesis of small gold clusters by reductive decomposition of $[Au(I)SR]_n$, bridging the gap between gold(I) thiolate complexes and thiolate-protected gold nanocrystals.[19] Nakamoto et al. have proved that thermolysis of gold(I) thiolate complexes can regulate the growth of gold nuclei and afford novel GNP passivation by alkyl groups.[20] In spite of these researches, few work was reported concerning the way to control the composition of $[Au(I)SR]_n$ that may create opportunities to directly tailor the properties of GNPs.[19,21]

$[Au(I)SR]_n$ is usually precipitated from the intermediate solutions by the BSM, and it has been shown to be insoluble in common solvents because of the intermolecular interactions between adjacent units. Different analysis techniques, such as X-ray diffraction, transmission electron microscopy, and Fourier transform IR spectroscopy, were introduced to characterize the crystal structures of such metal complexes.[14,22,26−28] To study the composition of the solid precipitates of gold thiolates, more characterization techniques are needed. Solid-state NMR (SSNMR) is an effective characterization technique for insolvable systems.[29−32] Reven and Lennox et al. successfully utilized SSNMR to characterize the structure, conformational, and dynamic properties of molecules on GNPs.[33−35] In our previous studies, we proved that, by using fast magic angle spinning (MAS, spinning speed ν_R > 20 kHz), high-resolution

Received: January 29, 2014
Revised: April 17, 2014
Published: April 21, 2014

^{1}H SSNMR spectra of solid samples could be obtained.[36−40] This technique is utilized here to characterize the structure of $[Au(I)SR]_n$.

In this paper, a series of gold thiolates capped with benzyl mercaptan (BM), $[Au(I)SC_7H_7]_n$, were prepared by precipitating from the intermediate solutions during the synthesis of GNPs by the BSM. The preparation of the precursor species before precipitation was monitored by UV and solution ^{1}H NMR spectroscopies. Gold(I) thiolates precipitated from these solutions were characterized by ^{1}H SSNMR under fast MAS, Raman spectroscopy, and thermogravimetric analysis (TGA). To study how to control the formation of gold thiolates, both 1-octadecanethiol ($C_{18}H_{37}SH$) and BM (C_7H_7SH) were used to form gold thiolates with mixed composition. The experimental results showed that the composition of $[Au(I)SR]_n$ can be controlled by changing the order of addition of C_7H_7SH and $C_{18}H_{37}SH$. This work can provide ways to prepare GNPs with desirable size and objective composition.

EXPERIMENTAL SECTION

Materials. Tetraoctylammonium bromide (TOAB 98%), sodium borohydride ($NaBH_4$ 99%), hydrogen tetrachloroaurate ($HAuCl_4{\cdot}4H_2O$), 1-octadecanethiol ($C_{18}H_{37}SH$), and BM (C_7H_7SH) were purchased from Sigma−Aldrich. Deuterated toluene was purchased from Alfa Aesar. All of the solvents were commercially available and distilled before use. All glassware was cleaned with aqua regia (HCl/HNO_3 = 3:1 vol %), rinsed with copious amounts of nanopure water, and then, dried in an oven prior to use.

Sample Preparation. The intermediate solutions were prepared by a typical two-phase BSM. An aqueous solution of $HAuCl_4{\cdot}4H_2O$ (22.5 mL, 30 mmol/L, 1 equiv) was mixed with a solution of TOAB in deuterated chloroform (60 mL, 50 mmol/L, 4.5 equiv). The two-phase mixture was rapidly stirred until Au^{3+} was all transferred to the organic phase to give a wine-red solution. After discarding the aqueous phase, we obtained the $[TOA][AuX_4]$ solution in deuterated chloroform. The solution was divided into six equal parts. After sufficient stirring, BM was added to each of six separated 10 mL deuterated chloroform solutions (1, 2, 3, 4, 5, and 7 equiv relative to the $[TOA][AuX_4]$ in each sample) to form intermediate solutions. Each sample was stirred for about 2 h to ensure the reaction completed, and corresponding ^{1}H NMR spectra were recorded.

Methanol was used to precipitate the gold thiolates from the reaction system. For the system with 1 and 2 equiv of thiol, no precipitate was found. For the sample with 3, 4, or more equiv, a large amount of precipitate was recognized after adding methanol. All of the gold thiolate precipitates were washed carefully with methanol and toluene for six times and dried afterward.

Characterization. Surface enhanced Raman scattering (SERS) experiments were performed on a Bruker MultiRAM with a 1064 nm Nd/YAG laser source and a Ge detector. The spectra were collected with a laser power of 10 mW and scan times of 400 if not specified.

One-dimensional solution ^{1}H NMR spectra were obtained on an AV-400 NMR spectrometer (Bruker BioSpin, Coventy, UK), equipped with a 5 mm PABBO BB probe, and operated at 400.13 MHz with a sample temperature of 25 °C.

^{1}H SSNMR experiments were performed on a Varian Infinityplus-400 wide-bore (89 mm) NMR spectrometer at a proton frequency of 399.7 MHz. A 2.5 mm T3 double-resonance CPMAS probe was used for ^{1}H SSNMR experiments, and it can provide stable spinning up to 30 kHz within ±2 Hz using a zirconia PENCIL rotor. The MAS frequency used in our experiments was 25 kHz. The ^{1}H chemical shifts were referenced to external TMS. The 90° pulse width was 1.4 μs. The recycle delay between two scans was set to 6 s, and each spectrum was acquired with 32 scans. The background signal was separately collected under the same condition with an empty rotor and then subtracted from the spectra acquired with samples in the same rotor. All of the NMR data were processed with Varian Spinsight software, and all experiments were carried out at room temperature.

TGA was performed on a PerKinElmer instrument, Pyris 1 TGA. Accurately weighed samples of 2−3 mg were run from room temperature to 700 °C at a rate of 20 °C/min under nitrogen (100 mL/min).

UV−visible (UV−vis) spectra were recorded with a UV1800PC UV−vis spectrophotometer operating at 1 nm resolution. The width of sample cuvette was 10 mm.

RESULTS AND DISCUSSION

An intermediate solution was obtained by mixing and stirring a 1:3 mol ratio $HAuCl_4{\cdot}4H_2O$ aqueous solution and TOAB in toluene and discarding the aqueous phase. After removing the solvents and redissolving in deuterated chloroform, BM of different equivalents was added. For investigating the precursor species, both UV and solution ^{1}H NMR spectroscopies are adopted. As shown in Figure 1, with increasing the amount of

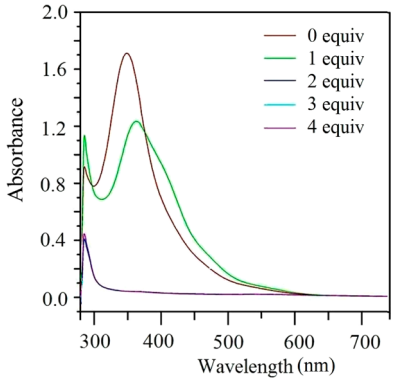

Figure 1. UV−vis absorption spectra for the titration of BM into a solution of $[TOA][AuX_4]$ and TOAX.

thiols, the intensity of the absorption band at 350 nm decreased and then disappeared when the amount of thiol reached 2 equiv or more. The disappearance of the 350 nm band indicated the complete reduction from Au(III) to Au(I), and it could be reasonably proposed that the initial 2 equiv of thiols act as the reductant in the reaction. We can see that complete reduction from Au(III) to Au(I) occurs with the addition of 2 equiv of thiols because the absorption band at 350 nm disappears after the addition of 2 equiv of thiols, so we propose that the former 2 equiv of thiols acts as the reductant in the reaction.

Utilizing solution ^{1}H NMR, more detailed information about the reactions between TOAX + $[TOA][AuX_4]$ and BM could be extracted, as shown in Figure 2. According to the ^{1}H NMR result in Figure 2, TOAB did not react with BM due to the appearance of two significant peaks of BM in Figure 2H (αCH_2 doublet at ca. 3.73 ppm and SH triplet at ca. 1.75 ppm). This result provides the evidence that the added thiols will not react

dx.doi.org/10.1021/jp501020k | J. Phys. Chem. C 2014, 118, 10434−10440

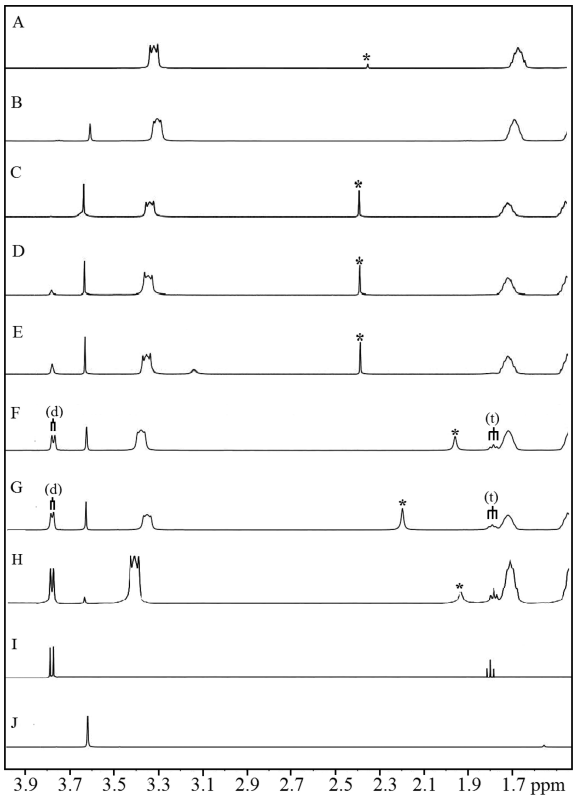

Figure 2. ^{1}H NMR spectra of TOAX + [TOA][AuX_4] solution with (A) 0, (B) 1, (C) 2, (D) 3, (E) 4, (F) 5, and (G)7 equiv of BM. For comparison, the ^{1}H NMR spectra of (H) a mixture of BM and TOAB, (I) BM, and (J) benzyl disulfide are also shown. * indicates water and solvent peaks.

with excess TOAB. Then, by integral calculation, it is found that, after adding 1 equiv of BM (Figure 2B), 0.5 equiv of benzyl disulfide is generated by reductive reaction (αCH_2 sharp singlet at ca. 3.60 ppm). Furthermore, the addition of 2 equiv of BM results in an increased amount of disulfide, indicating the continuous reduction. Further analysis also shows that the increasing amount is just as much as 0.5 equiv of disulfide. Subsequently, after the addition of 3 and 4 equiv of the thiols, a new peak at around 3.78 ppm appears, which has a little shift compared with the peak of BM. This peak is very probably the characteristic peak of αCH_2 bonded with Au(I). Meanwhile, no characteristic doublet peaks of free thiol are observed in Figure 2D, E. This means that no excess free thiols exist in the system when we add 3 and 4 equiv of BM. Also, by NMR integration analysis, it is found that the peak area of approximately 3.78 ppm in Figure 2E is twice as much as that in Figure 2D. The quantitative analysis provides a strong proof that two more equivalents of thiol reacts with the [TOA][AuX_2] complex. Finally, after adding 5 and 7 equiv of the thiol, Figure 2F, G shows the evidence of excess free thiols in the system (αCH_2 doublet at ca. 3.75 ppm and SH triplet at ca. 1.75 ppm). In conclusion, the liquid ^{1}H NMR spectra clearly shows that the third and forth equiv of thiols are involved in the reaction with [TOA][AuX_2].

When we precipitated the intermediates from the reaction system (1, 2, 3, and 4 equiv of thiol relative to the Au precursor) by adding methanol, no precipitate was produced unless there are 3 equiv and above of thiol in the reaction solutions. This phenomenon convincingly suggested that some new species of intermediates was produced when 3 equiv or more of thiol was added. We then washed the precipitate carefully with methanol and toluene several times and dried it afterward. Finally, we obtained a white solid precipitate. We then used ^{1}H SSNMR and Raman spectroscopies to analyze the precipitate, as shown in Figures 3 and 4. In Figure 3, ^{1}H

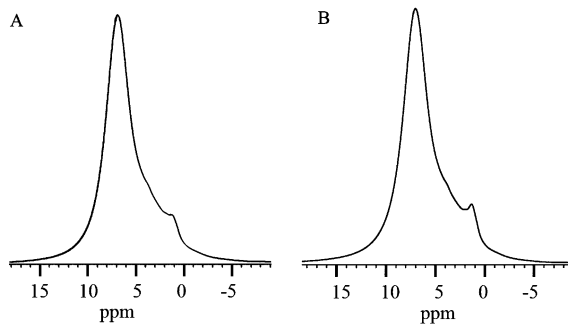

Figure 3. ^{1}H SSNMR spectra under MAS of precipitate from solution with 1 equiv of [TOA][AuX_4] and (A) 3 equiv of BM and (B) 4 equiv of BM.

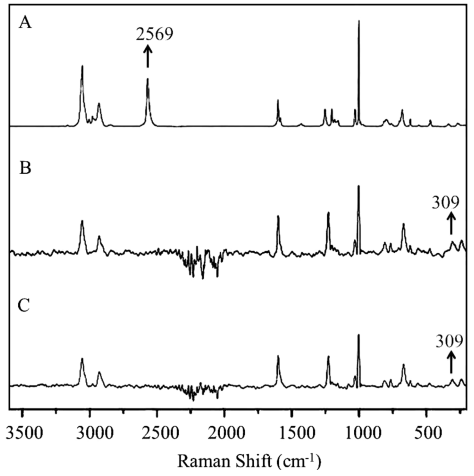

Figure 4. Raman spectra of (A) BM, (B) precipitate from solution with 1 equiv of [TOA][AuX_4] and 3 equiv of BM, and (C) precipitate from solution with 1 equiv of [TOA][AuX_4] and 4 equiv of BM.

SSNMR shows that the precipitate only has the component of BM and is very pure, as the spectra did not change with different amount of thiol. The chemical shifts of aromatic and methylene protons are observed at 7.0 and 1.5 ppm, respectively. The result of the Raman experiment in Figure 4 confirms that the precipitate has the component of BM. The disappearance of the S−H vibration at 2569 cm^{-1} and the new tiny peak at around 309 cm^{-1} of Au−S bond mercaptan demonstrates convincingly that the [Au(I)SR]$_n$-like polymer is formed when 3 and 4 equiv of thiol are added.

TGA analysis was also done for the precipitates obtained from the two different intermediate solutions, as shown in Figure 5. The two curves almost completely coincide with each other, indicating that these two samples may have the same composition. The lowest onset decomposition temperature (T_{onset}) and the complete decomposition temperature (T_{cd}) are 190 and 245 °C, respectively for both precipitates. The amount of residue from TGA is 60%. The residue is clarified as gold metal from the selected area electron diffraction pattern observed during transmission electron microscopy and also

dx.doi.org/10.1021/jp501020k | J. Phys. Chem. C 2014, 118, 10434−10440

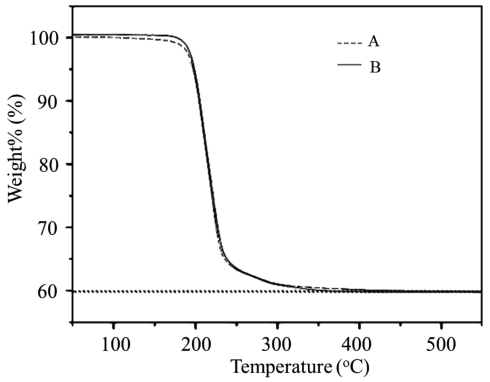

Figure 5. TGA result of precipitate from solution with 1 equiv of $[TOA][AuX_4]$ and (A) 3 equiv of BM and (B) 4 equiv of BM.

from the golden color of the material by Cha et al.[14] The amount of weight lost, 40%, should be ascribed to $-SC_7H_7$. According to the calculated result, the chemical formula of the molecular unit should be $[AuSC_7H_7]$.

For further verification, we also designed another reaction to prove our point. On the basis of the conclusion that 4 equiv of thiols was needed to complete the reaction with $[TOA][AuX_4]$, we designed a series of experiment to elucidate essential elements for determining the final composition of gold thiols. We changed the ratio and addition order of C_7H_7SH and $C_{18}H_{37}SH$ (4 equiv in total relative to the $[TOA][AuX_4]$).

By comparing Figure 6A–D, Figure 6C only shows the characteristic peaks of CH_2 of BM that is similar to Figure 6A. Figure 6D shows only characteristic peaks of CH_2 of $C_{18}H_{37}SH$ that was similar to Figure 6B although the ratio of BM and $C_{18}H_{37}SH$ was 2:2 (added in opposite sequence) in both of them, which should be due to the fact that the last two

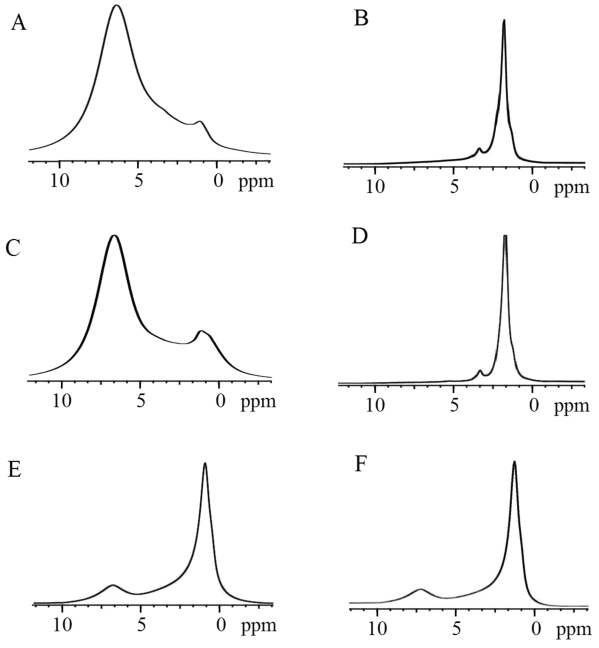

Figure 6. ^1H SSNMR spectra of the precipitate from solution with 1 equiv $[TOA][AuX_4]$ and (A) 4 equiv of BM, (B) 4 equiv of $C_{18}H_{37}SH$, (C) 2 equiv of $C_{18}H_{37}SH$ then 2 equiv of BM, (D) 2 equiv of BM then 2 equiv of $C_{18}H_{37}SH$, (E) 3 equiv of $C_{18}H_{37}SH$ then 1 of equiv BM, and (F) 3 equiv of BM then 1 equiv of $C_{18}H_{37}SH$.

equivalents of thiols added in were completely different. Figure 6E, F had the same spectrum, which contained characteristic peaks of CH_2 of both BM and 1-octadecanethiol, because the last two equivalents in the four equivalents of thiols added contained 1 equiv of BM and 1 equiv of 1-octadecanethiol. It may be concluded that the first two equivalents of thiols were not involved in the formation of gold thiolate.

Raman experiments (Figures 7 and 8) further proved this point. Comparing Figure 7A with B, it is found that the S–H

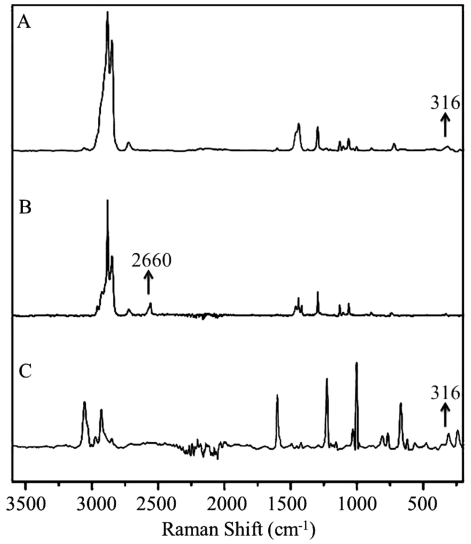

Figure 7. Raman spectra of the precipitate from solution with 1 equiv of $[TOA][AuX_4]$ and (A) 2 equiv of BM and 2 equiv of $C_{18}H_{37}SH$ (added in turn), (B) bulk $C_{18}H_{37}SH$, and (C) 2 equiv of $C_{18}H_{37}SH$ and 2 equiv of BM (added in turn).

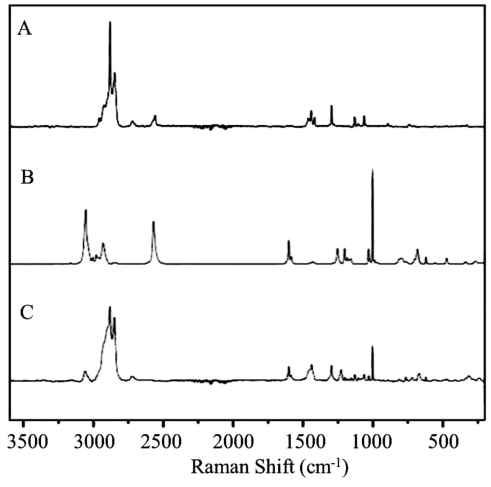

Figure 8. Raman spectra of the precipitate from solution with 1 equiv of $[TOA][AuX_4]$ and (A) bulk $C_{18}H_{37}SH$, (B) bulk BM, and (C) 3 equiv of BM and 1 equiv of $C_{18}H_{37}SH$ (added in turn).

vibration at 2660 cm^{-1} disappears and a new peak at 316 cm^{-1} appears. This result suggests that the $[Au(I)SC_{18}H_{37}]_n$-like polymer is very likely formed when two more equivalents of $C_{18}H_{37}SH$ is added. Also, from Figures 7 and 8, it is concluded that the final composition of the product is determined by order of addition of raw materials. The thiol added later is involved in the reaction of forming the $[Au(I)SR]_n$-like polymer, and it can be detected in the precipitate.

dx.doi.org/10.1021/jp501020k | J. Phys. Chem. C 2014, 118, 10434–10440

According to Figure 9, the curves of precipitates from solutions A and B are different completely, which means that

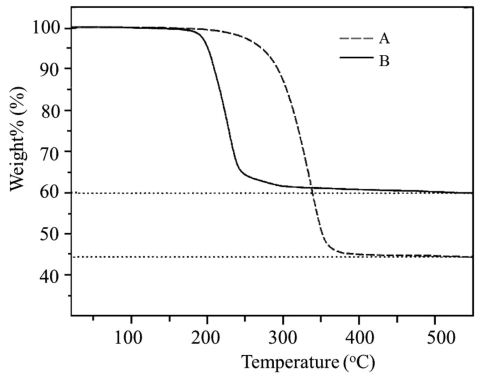

Figure 9. TGA result of precipitate from solution with 1 equiv of $[TOA][AuX_4]$ and (A) 2 equiv of BM and 2 equiv of $C_{18}H_{37}SH$ (added in turn), (B) 2 equiv of $C_{18}H_{37}SH$ and 2 equiv of BM (added in turn).

their composition is different. For precipitates from solution A, the lowest onset decomposition temperature (T_{onset}) and complete decomposition temperature (T_{cd}) are 240 and 360 °C, respectively. The amount of residue from TGA was 44.5%. For precipitates from solution B, the lowest onset decomposition temperature (T_{onset}) and complete decomposition temperature (T_{cd}) are 190 and 245 °C, respectively. The amount of residue from TGA is 60%.The results agree with those in Figure 5. In the same way as that according to Figure 5, we calculate the chemical formula of the molecular unit should be $[AuSC_{18}H_{37}]$ and $[AuSC_7H_7]$ for precipitates from A and B, respectively.

According to Figure 10, the precipitates show the lowest onset decomposition temperature (T_{onset}) and complete

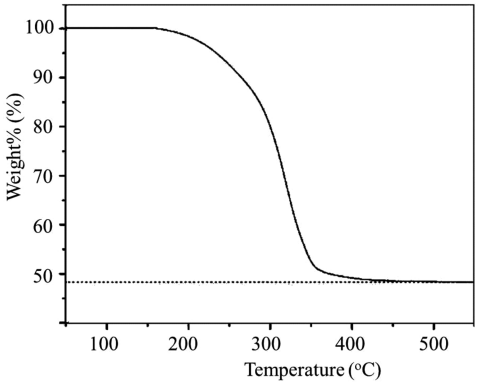

Figure 10. TGA result of the precipitate from solution with 1 equiv of $[TOA][AuX_4]$ and then 3 equiv of BM and 1 equiv of $C_{18}H_{37}SH$.

decomposition temperature (T_{cd}) as 200 and 350 °C, respectively. The amount of residue from TGA was 48%. In the same way, the calculated molecular formula is $[Au(SC_7H_7)_{0.5}(SC_{18}H_{37})_{0.5}]$. These results are perfectly consistent with the Raman result, and the Au−S bond is undoubtedly formed in the synthesized process.

Furthermore, the color of the three kinds of precipitates (yellow for $[Au(I)SC_7H_7]_n$, pale yellow for $[Au(I)SC_{18}H_{37}]_n$, and white for $[Au(I)SC_7H_7SC_{18}H_{37}]_n$ shows that the precipitate with both BM and $C_{18}H_{37}SH$ is not the simple mixture of the precipitate with BM and the precipitate with $C_{18}H_{37}SH$. This result supports strongly that the structure of the $[Au(I)SR]_n$-like polymer exists and the $[Au(I)SC_7H_7SC_{18}H_{37}]_n$-like polymer seems very likely the copolymer with BM and $C_{18}H_{37}SH$.

Polymeric $[Au(I)SR]_n$ was considered to be the intermediate Au(I) ion precursor during the Brust−Schiffrin two-phase synthesis of GNPs. Until recently Lennox and Tong et al.[8,15,17] showed that tetraoctyl-ammonium Au(I) halide complexes were actually the intermediate when the aqueous phase was removed. We monitored the change of the NMR spectra of the intermediate solutions and found precipitates $[Au(I)SR]_n$ formed gradually if the reaction solution was kept at room temperature for a few days (Supporting Information). During the real synthesis procedure, we usually could not observe the precipitates that also indicated $[Au(I)SR]_n$ did not form. The intermediate tetraoctyl-ammonium Au(I) halide complexes are then reduced to GNPs that always have residual surfactant TOAB coadsorbed on the surface while GNPs prepared from $[Au(I)SR]_n$ could obtain pure nanoparticles. In addition, it is difficult to tailor the composition of adsorbed species on GNPs by using the traditional BSM. Here, we successfully controlled the component of $[Au(I)SR]_n$ by changing the adding order of different thiols. They have great potential to be adapted to synthesize nanoparticles with binary ligands(molar ratio is around 1:1).

CONCLUSION

In summary, the preparation process of gold thiolates was clearly monitored by solution ^1H NMR, which showed that 4 equiv of thiols needed to complete the reaction. UV and ^1H NMR results showed that the first and second equivalents of thiols can reduce Au(III) to Au(I) completely. The third and fourth equivalents of thiols were then involved in the formation of $[Au(I)SR]_n$. According to the ^1H SSNMR, Raman, and TGA results, the composition of $[Au(I)SR]_n$ can be controlled by adjusting the species of the last two equivalents of thiols, which also provides the possibility to regulate the adsorbed species on GNPs. More functional GNPs can be well produced and thus be applied into the field of biochemistry and surface science.

ASSOCIATED CONTENT

Supporting Information

Additional NMR spectra. This material is available free of charge via the Internet at http://pubs.acs.org.

AUTHOR INFORMATION

Corresponding Authors

*(X.W.) E-Mail: wangxiaoliang@nju.edu.cn.
*(G.X.) E-mail: xuegi@nju.edu.cn.

Notes

The authors declare no competing financial interest.

ACKNOWLEDGMENTS

We gratefully acknowledge National Basic Research Program of China (973 Program, 2012 CB 821503), the National Science Foundation of China (nos. 51133002, 21174062, 21274060, 21274059, and 21074052), the foundation research project of Jiangsu province (BK20131269), Program for Changjiang Scholars, and Innovative Research Team in University.

REFERENCES

(1) Brust, M.; Walker, M.; Bethell, D.; Schiffrin, D. J.; Whyman, R. Synthesis of Thiol-Derivatized Gold Nanoparticles in a Two-Phase Liquid-Liquid System. *J. Chem. Soc., Chem. Commun.* **1994**, 801−802.

(2) Murray, R. W. Nanoelectrochemistry: Metal Nanoparticles, Nanoelectrodes, and Nanopores. *Chem. Rev.* **2008**, *108*, 2688−2720.

(3) Daniel, M. C.; Astruc, D. Gold Nanoparticles: Assembly, Supramolecular Chemistry, Quantum-Size-Related Properties, and Applications toward Biology, Catalysis, and Nanotechnology. *Chem. Rev.* **2004**, *104*, 293−346.

(4) Sardar, R.; Funston, A. M.; Mulvaney, P.; Murray, R. W. Gold Nanoparticles: Past, Present, and Future. *Langmuir* **2009**, *25*, 13840−13851.

(5) Badia, A.; Singh, S.; Demers, L.; Cuccia, L.; Brown, G. R.; Lennox, R. B. Self-Assembled Monolayers on Gold Nanoparticles. *Chem.—Eur. J.* **1996**, *2*, 359−363.

(6) Bunz, U. H. F.; Rotello, V. M. Gold Nanoparticle-Fluorophore Complexes: Sensitive and Discerning "Noses" for Biosystems Sensing. *Angew. Chem., Int. Ed.* **2010**, *49*, 3268−3279.

(7) Caseri, W. Nanocomposites of Polymers and Metals or Semiconductors: Historical Background and Optical Properties. *Macromol. Rapid Commun.* **2000**, *21*, 705−722.

(8) Goulet, P. J. G.; Lennox, R. B. New Insights into Brust-Schiffrin Metal Nanoparticle Synthesis. *J. Am. Chem. Soc.* **2010**, *132*, 9582−9584.

(9) Barngrover, B. M.; Aikens, C. M. Electron and Hydride Addition to Gold(I) Thiolate Oligomers: Implications for Gold-Thiolate Nanoparticle Growth Mechanisms. *J. Phys. Chem. Lett.* **2011**, *2*, 990−994.

(10) Susha, A. S.; Ringler, M.; Ohlinger, A.; Paderi, M.; LiPira, N.; Carotenuto, G.; Rogach, A. L.; Feldmann, J. Strongly Luminescent Films Fabricated by Thermolysis of Gold-Thiolate Complexes in a Polymer Matrix. *Chem. Mater.* **2008**, *20*, 6169−6175.

(11) Cha, S. H.; Kim, J. U.; Kim, K. H.; Lee, J. C. Preparation and Photoluminescent Properties of Gold(I)-Alkanethiolate Complexes Having Highly Ordered Supramolecular Structures. *Chem. Mater.* **2007**, *19*, 6297−6303.

(12) Schaaff, T. G.; Knight, G.; Shafigullin, M. N.; Borkman, R. F.; Whetten, R. L. Isolation and Selected Properties of a 10.4 kDa Gold: Glutathione Cluster Compound. *J. Phys. Chem. B* **1998**, *102*, 10643−10646.

(13) Templeton, A. C.; Chen, S. W.; Gross, S. M.; Murray, R. W. Water-Soluble, Isolable Gold Clusters Protected by Tiopronin and Coenzyme A Monolayers. *Langmuir* **1999**, *15*, 66−76.

(14) Cha, S. H.; Kim, K. H.; Kim, J. U.; Lee, W. K.; Lee, J. C. Thermal Behavior of Gold(I)-Thiolate Complexes and Their Transformation into Gold Nanoparticles under Heat Treatment Process. *J. Phys. Chem. C* **2008**, *112*, 13862−13868.

(15) Li, Y.; Zaluzhna, O.; Xu, B. L.; Gao, Y. A.; Modest, J. M.; Tong, Y. J. Mechanistic Insights into the Brust-Shiffrin Two-Phase Synthesis of Organo-Chalcogenate-Protected Metal Nanoparticles. *J. Am. Chem. Soc.* **2011**, *133*, 2092−2095.

(16) Li, Y.; Zaluzhna, O.; Xu, B. L.; Gao, Y.; Modest, J. M.; Tong, Y. J. Mechanistic Insights into the Brust-Schiffrin Two-Phase Synthesis of Organo-Chalcogenate-Protected Metal Nanoparticles (Addition/Correction; vol 133, pg 2092, 2011). *J. Am. Chem. Soc.* **2012**, *134*, 6498−6498.

(17) Li, Y.; Zaluzhna, O.; Tong, Y. Y. J. Critical Role of Water and the Structure of Inverse Micelles in the Brust-Schiffrin Synthesis of Metal Nanoparticles. *Langmuir* **2011**, *27*, 7366−7370.

(18) Li, Y.; Zaluzhna, O.; Tong, Y. Y. J. Identification of a Source of Size Polydispersity and Its Solution in Brust-Schiffrin Metal Nanoparticle Synthesis. *Chem. Commun.* **2011**, *47*, 6033−6035.

(19) Negishi, Y.; Nobusada, K.; Tsukuda, T. Glutathione-Protected Gold Clusters Revisited: Bridging the Gap between Gold(I)-Thiolate Complexes and Thiolate-Protected Gold Nanocrystals. *J. Am. Chem. Soc.* **2005**, *127*, 5261−5270.

(20) Nakamoto, M.; Yamamoto, M.; Fukusumi, M. Thermolysis of Gold(I) Thiolate Complexes Producing Novel Gold Nanoparticles Passivated by Alkyl Groups. *Chem. Commun.* **2002**, 1622−1623.

(21) Brinas, R. P.; Hu, M. H.; Qian, L. P.; Lymar, E. S.; Hainfeld, J. F. Gold Nanoparticle Size Controlled by Polymeric Au(I) Thiolate Precursor Size. *J. Am. Chem. Soc.* **2008**, *130*, 975−982.

(22) Corbierre, M. K.; Lennox, R. B. Preparation of Thiol-Capped Gold Nanoparticles by Chemical Reduction of Soluble Au(I)-Thiolates. *Chem. Mater.* **2005**, *17*, 5691−5696.

(23) Barngrover, B. M.; Aikens, C. M. The Golden Pathway to Thiolate-Stabilized Nanoparticles: Following the Formation of Gold-(I) Thiolate from Gold(III) Chloride. *J. Am. Chem. Soc.* **2012**, *134*, 12590−12595.

(24) Reilly, S. A.; Krick, T.; Dass, A. Surfactant-Free Synthesis of Ultrasmall Gold Nanoclusters. *J. Phys. Chem. C* **2010**, *114*, 741−745.

(25) Jin, R. C. Quantum Sized, Thiolate-Protected Gold Nanoclusters. *Nanoscale* **2010**, *2*, 343−362.

(26) Parikh, A. N.; Gillmor, S. D.; Beers, J. D.; Beardmore, K. M.; Cutts, R. W.; Swanson, B. I. Characterization of Chain Molecular Assemblies in Long-Chain, Layered Silver Thiolates: A Joint Infrared Spectroscopy and X-ray Diffraction Study. *J. Phys. Chem. B* **1999**, *103*, 2850−2861.

(27) Pyykko, P. Theoretical Chemistry of Gold. *Angew. Chem., Int. Ed.* **2004**, *43*, 4412−4456.

(28) Hunks, W. J.; Jennings, M. C.; Puddephatt, R. J. Polymeric and Macrocyclic Gold(I) Complexes with Bridging Dithiolate and Diphosphine Ligands. *Inorg. Chim. Acta* **2006**, *359*, 3605−3616.

(29) Schmitt, H.; Badia, A.; Dickinson, L.; Reven, L.; Lennox, R. B. The Effect of Terminal Hydrogen Bonding on the Structure and Dynamics of Nanoparticle Self-Assembled Monolayers (SAMs): An NMR Dynamics Study. *Adv. Mater.* **1998**, *10*, 475−480.

(30) Calucci, L.; Forte, C.; Galleschi, L.; Geppi, M.; Ghiringhelli, S. ^{13}C and ^{1}H Solid State NMR Investigation of Hydration Effects on Gluten Dynamics. *Int. J. Biol. Macromol.* **2003**, *32*, 179−189.

(31) Guo, M. M. Solid-State High-Resolution NMR Studies on the Miscibility of Polymer Blends. *Trends Polym. Sci.* **1996**, *4*, 238−244.

(32) Egger, N.; Schmidt-Rohr, K.; Blumich, B.; Domke, W. D.; Stapp, B. Solid-State NMR Investigation of Cationic Polymerized Epoxy-Resins. *J. Appl. Polym. Sci.* **1992**, *44*, 289−295.

(33) Fiurasek, P.; Reven, L. Phosphonic and Sulfonic Acid-Functionalized Gold Nanoparticles: A Solid-State NMR Study. *Langmuir* **2007**, *23*, 2857−2866.

(34) Badia, A.; Cuccia, L.; Demers, L.; Morin, F.; Lennox, R. B. Structure and Dynamics in Alkanethiolate Monolayers Self-Assembled on Gold Nanoparticles: A DSC, FT-IR, and Deuterium NMR Study. *J. Am. Chem. Soc.* **1997**, *119*, 2682−2692.

(35) Badia, A.; Demers, L.; Dickinson, L.; Morin, F. G.; Lennox, R. B.; Reven, L. Gold-Sulfur Interactions in Alkylthiol Self-Assembled Monolayers Formed on Gold Nanoparticles Studied by Solid-State NMR. *J. Am. Chem. Soc.* **1997**, *119*, 11104−11105.

(36) Zhu, L. L.; Zhang, C.; Guo, C. C.; Wang, X. L.; Sun, P. C.; Zhou, D. S.; Chen, W.; Xue, G. New Insight into Intermediate Precursors of Brust-Schiffrin Gold Nanoparticles Synthesis. *J. Phys. Chem. C* **2013**, *117*, 11399−11404.

(37) Wang, X. L.; Tao, F. F.; Sun, P. C.; Zhou, D. S.; Wang, Z. Q.; Gu, Q.; Hu, J. L.; Xue, G. Probing Chain Interpenetration in Polymer Glasses by H-1 Dipolar Filter Solid-State NMR under Fast Magic Angle Spinning. *Macromolecules* **2007**, *40*, 4736−4739.

(38) Zhu, L. L.; Gu, Q.; Sun, P. C.; Chen, W.; Wang, X. L.; Xue, G. Characterization of the Mobility and Reactivity of Water Molecules on TiO_2 Nanoparticles by ^{1}H Solid-State Nuclear Magnetic Resonance. *ACS Appl. Mater. Interfaces* **2013**, *5*, 10352−10356.

(39) Wang, X. L.; Gu, Q.; Sun, Q.; Zhou, D. S.; Sun, P. C.; Xue, G. Characterization of Polymer Compatibility by ^{1}H Dipolar Filter Solid-State NMR under Fast Magic Angle Spinning. *Macromolecules* **2007**, *40*, 9018−9025.

(40) Chen, J.; Xu, J.; Wang, X. L.; Zhou, D. S.; Sun, P. C.; Xue, G. Thickness Dependence of Glass Transitions Measured by AC-Chip

Calorimetry in Films with Controlled Interface. *Macromolecules* **2013**, *46*, 7006−7011.